Polarization mixing error in transmission ellipsometry with two acousto-optical modulators

Yuanlong Deng
Jinlong Chai
Xuejin Li
Yubin Wu
Gang Xu
ShenZhen University
College of Mechatronics & Control Engineering
ShenZhen Key Lab of Advanced
Mould-Manufacturing Technology
ShenZhen 518060, China.
E-mail: dengyL@szu.edu.cn

Abstract. A transmission ellipsometer with the configuration of modified Mach-Zehnder heterodyne interferometer is demonstrated. Two acousto-optical modulators are employed to generate a 20-kHz beat frequency. The scheme offers high resistance to environmental turbulence because of the interferometric components passing through the same path. A single layer of indium tin oxide on a glass substrate was measured, and an error up to several nanometers of the sample thickness is observed. The polarization mixing error is mainly due to the imperfection of polarizing beamsplitters (PBSs) and to the elliptical polarization and nonorthogonality of the light beams produced by the laser source and wave plates. The mechanism governing the error and its influence on measurement accuracy is analyzed with the Jones matrix method. In contrast with interferometric reflection ellipsometry using a Zeeman laser, the theoretical analysis indicates that only second-order error is introduced in this system. The elliptical polarization and nonorthogonality, occurring only before the light splitting, have little influence on measurement accuracy; the imperfection of PBSs is the major contributor to the polarization mixing error. [DOI: 10.1117/1.2955770]

Subject terms: ellipsometry; heterodyne interferometry; film measurement; acousto-optical modulator; polarization mixing error.

Paper 080065R received Jan. 22, 2008; revised manuscript received Apr. 21, 2008; accepted for publication Apr. 23, 2008; published online Jul. 30, 2008.

1 Introduction

Many kinds of thin films with thickness on the order of nanometers have wide application in the fields of microelectronics, materials and chemical engineering, and optical and laser technology. The optical constants of thin and ultrathin films are of crucial importance to the products' performance.[1] Having the advantages of high precision, noncontact measurement, and the ability to determine both refractive index and thickness simultaneously, ellipsometry is one of the most powerful techniques for measuring the optical properties of thin films.[2] Ellipsometers today have been making much progress in automation in various ways and are widely used for *in situ* measurements.[1,3] However, they are still not suitable for application to very fast surface processes with millisecond or microsecond resolution.[4] In addition, in present ellipsometers some kinds of errors are inherent due to the mechanical rotation of optical components.[5] Mechanical rotation also limits the measurement speed.

Because of their noncontact nature, high resistance to environmental turbulence, low uncertainty, and high resolution, optical heterodyne interferometers have been developed for a variety of applications. By employing heterodyne interferometry, many researchers hope to make ellipsometers work at higher speeds and be more suitable for interferential environments. In principle this kind of new ellipsometers can be described as follows: linearly polarized light in the measurement arm of an interferometer is modulated by a film sample, and then recombines at a beamsplitter with light components from the reference arm. The composite light is spatially separated into p- and s-polarized components before being converted to electrical signals.

Hazebroke et al. produced two heterodyne signals by moving a corner-cube reflector in the reference arm at constant speed,[6,7] and obtained the ellipsometric parameters from the amplitudes and phase difference. However, the moving reflector driven by an electromechanical device led to some problems:[8] the beat frequency was not stable enough, and the process was as slow as 8 s per measurement. A possible solution to these problems, proposed by Wind et al., was to use a Zeeman laser to generate a beat frequency at 1 MHz.[8] Several different setups were compared and analyzed theoretically, but experimental data and errors of the heterodyne interferometry were not reported. Lin et al. used two acousto-optical modulators to produce a beat frequency at 49.4 kHz, and combined optical heterodyne and phase lock-in techniques to build up a reflection ellipsometry system, which they used to measure the refractive indexes of metal films.[5] Electro-optic modulators and wavelength-modulated laser diodes were also utilized to produce the beat frequency, and Michelson interferometers were employed to measure films with thicknesses of several hundred nanometers.[9,10] But the low beat frequencies produced by electro-optic modulators and wavelength-modulated laser diode limited the improvement of measurement speed. Though many new developments of interferometric ellipsometers have been reported, to our

0091-3286/2008/$25.00

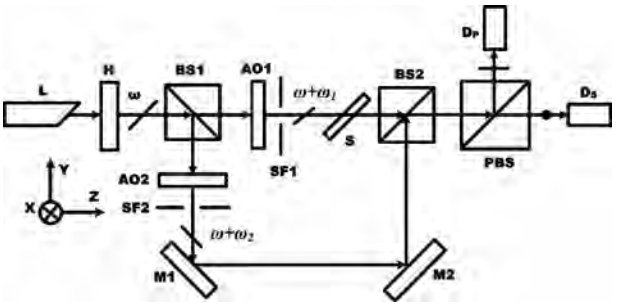

Fig. 1 Schematic of the optical configuration. L: He-Ne laser; H: half-wave plate; AO: acousto-optical modulators; SF: spatial filter; PBS: polarizing beamsplitters; M: mirrors; BS: beamsplitters; S: film sample; D: detector.

knowledge no further research on the polarization mixing error of interferometric ellipsometers has been reported.

Though heterodyne interferometers offer subnanometer resolution, their accuracy is limited by their nonlinearity.[11] A clearer understanding of the mechanism governing the error may lead to better compensation and elimination at minimal cost. Many reports have discussed the error;[11–18] however, they all addressed systems using either dynamic displacement or Michelson configurations incorporating Zeeman lasers, and several error terms were only discussed separately.

In this paper, a new configuration of interferometric transmission ellipsometry is introduced. Addressing the imperfection of polarizing beamsplitters (PBSs) and the resulting distortion of the polarization state of light beams, the polarization mixing error in heterodyne interferometric ellipsometers was calculated; its drifting can be used to explain the instability of the experimental results. For simplicity, this paper focuses only on nonabsorbing and isotropic thin films.

2 Theory and Experimental Setup

The experimental setup is a modified Mach-Zehnder interferometer, as Fig. 1 shows. A Uniphase model 1107P He-Ne laser emits linearly polarized light of wavelength 632.8 nm. It has 0.8-mW continuous output power, and its polarization ratio is up to 500:1. The laser beam is incident on a half-wave plate (H), which polarizes the transmitted beam at 45 deg to the *X* axis. A beamsplitter (BS1) splits the light into two equal-intensity arms, one for reference and the other for measurement. Two acousto-optical modulators (Model AOM-40, IntraAction Corp.) driven by a dual-frequency source (Model DFE-A4, IntraAction Corp.) are used as frequency shifters. The frequency difference is set at 20 kHz, i.e., $\Delta\omega=\omega_2-\omega_1=1.256\times10^5$ rad/s. The spatial filters are required to block zero-order waves. The p and s components of the measurement beam, with approximately equal intensity, are directed towards a film sample. After being modulated by the film sample, they recombine at BS2 with the corresponding components of the reference beam. After the polarizing beamsplitter (PBS) followed by two detectors, the p and s components are separated and two sinusoidal signals with a beat frequency $\Delta\omega$ are generated.

The light incident on BS1 may be represented as

$$E=\begin{pmatrix}1\\1\end{pmatrix}\exp[i(\omega t+\alpha)]. \tag{1}$$

Here α is the initial phase. By using the Jones matrix method, the response of optical system can be easily described. The electric field components of the beams incident on the photodetectors D_p and D_s are, respectively,

$$\begin{aligned}E_P=P_R\Bigg[&B_TS_TB_T\begin{pmatrix}1\\1\end{pmatrix}\exp\{i[(\omega+\omega_1)t+\alpha_1]\}\\&+B_RMMB_R\begin{pmatrix}1\\1\end{pmatrix}\exp\{i[(\omega+\omega_2)t+\alpha_2]\}\Bigg],\\E_S=P_T\Bigg[&B_TS_TB_T\begin{pmatrix}1\\1\end{pmatrix}\exp\{i[(\omega+\omega_1)t+\alpha_1]\}\\&+B_RMM\cdot B_R\cdot\begin{pmatrix}1\\1\end{pmatrix}\exp\{i[(\omega+\omega_2)t+\alpha_2]\}\Bigg].\end{aligned} \tag{2}$$

Here α_1 and α_2 are new initial phases, the subscripts R and T mean reflection and transmission, and the *P*, *B*, *M*, and *S* represent the Jones matrices of the polarizing beamsplitter, beamsplitters, mirrors, and film sample, respectively,

$$\begin{aligned}&P_R=\begin{pmatrix}0&0\\0&1\end{pmatrix},\quad P_T=\begin{pmatrix}1&0\\0&0\end{pmatrix},\quad B_R=B_T=\frac{1}{2}\begin{pmatrix}1&0\\0&1\end{pmatrix},\\&S_T=\begin{pmatrix}t_S&0\\0&t_P\end{pmatrix},\quad M=\begin{pmatrix}1&0\\0&-1\end{pmatrix}\end{aligned} \tag{3}$$

with

$$t_S=|t_S|\exp(i\phi_S),\qquad t_P=|t_P|\exp(i\phi_P) \tag{4}$$

Equation (4) gives the transmission coefficients of the sample for the p and s components, respectively.

Substitution of Eq. (3) and Eq. (4) into Eq. (2) gives

$$\begin{aligned}E_S&=\frac{1}{4}t_S\exp\{i[(\omega+\omega_1)t+\alpha_1]\}+\frac{1}{4}\exp\{i[(\omega+\omega_2)t+\alpha_2]\},\\E_P&=\frac{1}{4}t_P\exp\{i[(\omega+\omega_1)t+\alpha_1]\}+\frac{1}{4}\exp\{i[(\omega+\omega_2)t+\alpha_2]\}.\end{aligned} \tag{5}$$

Neglecting constant coefficients, the normalized signal intensities of the oscillating terms are obtained:

$$\begin{aligned}I_S&\propto|t_S|\cos(\Delta\omega\cdot t+\phi_S+\Delta\alpha),\\I_P&\propto|t_P|\cos(\Delta\omega\cdot t+\phi_p+\Delta\alpha).\end{aligned} \tag{6}$$

A calibration procedure is necessary for the measurement. By removing the film sample from the optical setup, the detection signals are obtained directly according to the preceding analysis:

$$I_S^c\propto\cos(\Delta\omega\cdot t+\Delta\alpha), \tag{7}$$

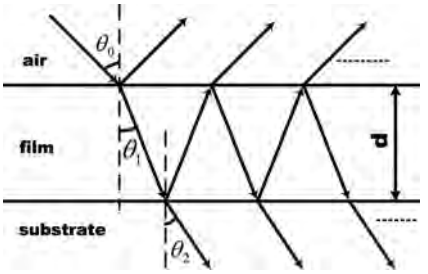

Fig. 2 Schematic of the air-film-substrate system (λ=632.8 nm, n_0=1.00, n_2=1.515, n_1=2.0, θ_0=75.0 deg).

$$I_P^c \propto \cos(\Delta\omega \cdot t + \Delta\alpha).$$

The pair of ellipsometric parameters $(\tan\psi, \Delta)$ can be derived from amplitude ratio and phase difference between I_S and I_P, i.e,

$$\Delta = [\phi(I_P) - \phi(I_P^c)] - [\phi(I_S) - \phi(I_S^c)] = \phi_P - \phi_S,$$
$$\tan\psi = |\rho| = \frac{A(I_P)}{A(I_P^c)} \Big/ \frac{A(I_S)}{A(I_S^c)} = |t_p|/|t_S|. \tag{8}$$

Here, the ϕ and A represent the phases and amplitudes of the optical intensity signals.

Theoretically speaking, the setup has the advantage of being immune to atmospheric disturbance because $\Delta\alpha$ in Eq. (6) does not affect the measurement accuracy.

3 Experimental Results

The film sample is indium tin oxide (ITO) on a glass substrate, as Fig. 2 shows. The spot diameter of the incident beam is about 1 mm. A scanning probe microscope (CSPM-4000, produced by Benyuan Co., Ltd., vertical resolution, 0.1 nm) with a silicon cantilever is employed to calibrate the film thickness. The calibration result at the tested point is 35.0 ± 0.5 nm. The experimental data on the same tested point and inversion results are given in Table 1. The error of film thickness measurement ranges up to 4 nm. This error, mainly introduced by polarization mixing, is discussed in detail below.

4 Analysis of Polarization Mixing Error

The nonlinearity of displacement or distance measurement systems using Michelson interferometers has been studied by many researchers.[11–18] To our knowledge, no researches on the polarization mixing error of interferometric transmission ellipsometry have been reported. There are two kinds of errors in heterodyne interferometers,[19] namely, frequency mixing error and polarization mixing error. Frequency mixing error is predominant; polarization mixing error tends to be smaller. In the system showed in Fig. 1, the frequency shifts are obtained separately inside of each arm by using two acousto-optical modulators instead of a Zeeman laser, so the frequency mixing error is expected to be avoided.

The polarization mixing error mainly arises from leakage of the PBS, elliptical polarization, and nonorthogonality as a result of imperfect or misoriented laser source, wave plates, beamsplitters and reflecting mirrors.[19] This paper restricts attention to two sources of measurement errors: (1) imperfections in the PBS and other components in the interferometer arms, and (2) ellipticity and nonorthogonality defects in the laser beam incident on the interferometer. Because we only consider relative phase and magnitude between the s and p components, the prefactors, which do not contribute to the discussion, are ignored in the following analysis.

Table 1 Experimental data for the single-layer ITO.

No.	$\lvert\rho\rvert$	Δ (deg)	n_1	d (nm)
1	1.566	−7.2	2.014	34.5
2	1.564	−7.4	2.072	37.4
3	1.570	−7.2	2.131	38.9
4	1.541	−7.5	1.941	35.0
5	1.566	−7.4	2.076	37.4
6	1.574	−7.1	2.037	34.3
7	1.555	−7.5	2.053	37.9
8	1.562	−7.4	2.069	37.6
9	1.558	−7.5	2.059	37.8
10	1.552	−7.6	2.045	38.1

The ideal polarization state of the light beam incident on BS1 in Fig. 3(a) can be described by Eq. (1). Because of the imperfection and misorientation of the laser source and the half-wave plate, the nonideal light incident on BS1, as shown in Fig. 3(b), actually is of elliptical polarization. Similarly to Eq. (1), in the x'-y' coordinate systems it is written as

$$E = \begin{pmatrix} 1 \\ b\exp\left[i\left(\frac{\pi}{2} - \varepsilon\right)\right] \end{pmatrix} \exp[i(\omega t + \alpha)]. \tag{9}$$

The ellipticity b is the ratio of minor to major axis, and ε represents the nonorthogonality. These can range up to 0.05 and 3 deg, respectively, even in many good metrology-grade laser sources.[13] The situation will be worse if imper-

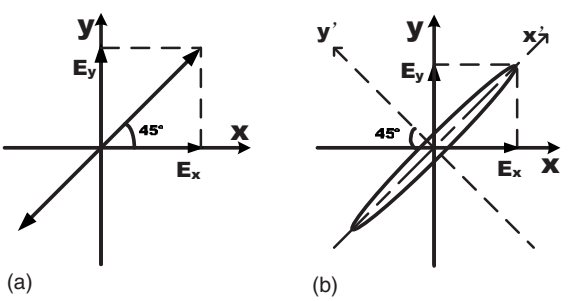

Fig. 3 (a) Ideal linearly polarized light. (b) Schematic of elliptical polarization.

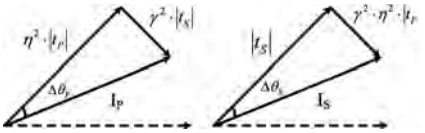

Fig. 4 Phasor diagram of error analysis.

fection and misalignment of the half-wave plate are considered.

In the x-y coordinate system Eq. (9) changes to

$$E = \begin{pmatrix} E_x \\ E_y \end{pmatrix} = \begin{pmatrix} 1 - ib\exp(i\varepsilon) \\ 1 + ib\exp(i\varepsilon) \end{pmatrix} \exp[i(\omega t + \alpha)]. \tag{10}$$

For simplicity, Eq. (10) can be replaced by the following normalized form after ignoring the prefactors:

$$E = \begin{pmatrix} E_x \\ E_y \end{pmatrix} = \begin{pmatrix} 1 \\ \eta\exp(i\beta) \end{pmatrix} \exp[i(\omega t + \alpha)]. \tag{11}$$

Here

$$\eta\exp(i\beta) = \frac{1 + b\sin\varepsilon - ib\cos\varepsilon}{1 - b\sin\varepsilon + ib\cos\varepsilon}. \tag{12}$$

Taking account of imperfection and misorientation, the Jones matrices of the PBS are modified as

$$P_T = \begin{pmatrix} 1 & 0 \\ 0 & \gamma \end{pmatrix}, \qquad P_R = \begin{pmatrix} \gamma & 0 \\ 0 & 1 \end{pmatrix} \tag{13}$$

Here γ represents the real extinction ratio of the PBS.

Substitution of Eq. (11) and (13) into Eq. (2) gives the field vectors on the photodetectors, as follows:

$$\begin{aligned} E_P = \begin{pmatrix} E_P^x \\ E_P^y \end{pmatrix} &\propto \begin{pmatrix} \gamma t_S \\ t_P \eta\exp(i\beta) \end{pmatrix} \exp\{i[(\omega + \omega_1)t + \alpha_1]\} \\ &+ \begin{pmatrix} \gamma \\ \eta\exp(i\beta) \end{pmatrix} \exp\{i[(\omega + \omega_2)t + \alpha_2]\}, \\ E_S = \begin{pmatrix} E_S^x \\ E_S^y \end{pmatrix} &\propto \begin{pmatrix} t_S \\ \gamma t_P \eta\exp(i\beta) \end{pmatrix} \exp\{i[(\omega + \omega_1)t + \alpha_1]\} \\ &+ \begin{pmatrix} 1 \\ \gamma\eta\exp(i\beta) \end{pmatrix} \exp\{i[(\omega + \omega_2)t + \alpha_2]\}. \end{aligned} \tag{14}$$

Then the normalized intensity signals on the photodetectors may be written as

$$\begin{aligned} I_P = I_P^x + I_P^y &\propto \gamma^2|t_S|\cos(\Delta\omega t + \phi_S + \Delta\alpha) \\ &+ \eta^2|t_P|\cos(\Delta\omega t + \phi_P + \Delta\alpha), \\ I_S = I_S^x + I_S^y &\propto |t_S|\cos(\Delta\omega t + \phi_S + \Delta\alpha) \\ &+ \gamma^2\eta^2|t_P|\cos(\Delta\omega t + \phi_P + \Delta\alpha). \end{aligned} \tag{15}$$

Because η is near 1 and γ is far smaller than 1, we have

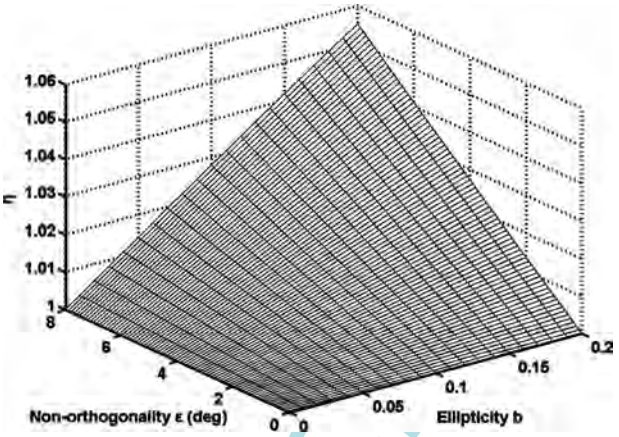

Fig. 5 Dependence of η on ellipticity b and non orthogonality ε.

$$I_P^y \gg I_P^x, \qquad I_S^x \gg I_S^y. \tag{16}$$

So we can use the method of vector addition to evaluate the effect of I_P^x and I_S^y, as Fig. 4 shows.

According to Fig. 4 and Eqs. (15) and (16), the extremal influence introduced by I_P^x and I_S^y can be described as

$$\begin{aligned} I_P &\approx (\gamma^2|t_S| + \eta^2|t_P|)\cos(\Delta\omega t + \phi_P \pm \Delta\theta_P + \Delta\alpha), \\ I_S &\approx (|t_S| + \gamma^2\eta^2|t_P|)\cos(\Delta\omega t + \phi_S \pm \Delta\theta_S + \Delta\alpha). \end{aligned} \tag{17}$$

Here

$$\begin{aligned} \Delta\theta_P &\approx \tan^{-1}\left(\frac{\gamma^2|t_S|}{\eta^2|t_P|}\right) \approx \frac{\gamma^2|t_S|}{\eta^2|t_P|}, \\ \Delta\theta_S &\approx \tan^{-1}\left(\frac{\gamma^2\eta^2|t_P|}{|t_S|}\right) \approx \frac{\gamma^2\eta^2|t_P|}{|t_S|}. \end{aligned} \tag{18}$$

Similarly, the calibration intensity signals without the film sample can be represented as

$$\begin{aligned} I_P' &= (\gamma^2 + \eta^2)\cos(\Delta\omega t + \Delta\alpha), \\ I_S' &= (1 + \gamma^2\eta^2)\cos(\Delta\omega t + \Delta\alpha). \end{aligned} \tag{19}$$

According to Eq. (8), now the errors in the ellipsometric parameters may be written as

$$\frac{\delta|\rho|}{|\rho|} = \left(\frac{\gamma^2|t_S| + \eta^2|t_P|}{\gamma^2 + \eta^2} \cdot \frac{1 + \gamma^2\eta^2}{|t_S| + \gamma^2\eta^2|t_P|}\right)\frac{|t_S|}{|t_P|} - 1, \tag{20}$$

$$\delta\Delta = |\Delta\theta_P| + |\Delta\theta_S|. \tag{21}$$

It is clear that the polarization mixing error cannot be eliminated just by a calibration procedure.

5 Discussion

We see in Eq. (15) that the phase β in Eq. (12) does not influence the measurement accuracy. Therefore, we find that η can be written as

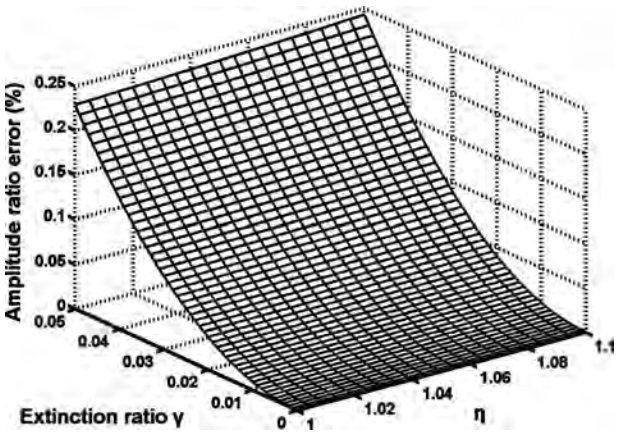

Fig. 6 Amplitude ratio error versus η and γ.

$$\eta = \left(\frac{1 + b^2 + 2b \sin \varepsilon}{1 + b^2 - 2b \sin \varepsilon}\right)^{1/2}. \tag{22}$$

Figure 5 shows the dependence of η on b (ellipticity) and ε (nonorthogonality). Substituting the sample specifications into into Eqs. (20) and (21), the ellipsometric parameters' polarization mixing errors produced by the imperfection of the PBS and the distortion of polarization state of light beams are found as shown in Figs. 6 and 7.

The errors in the ellipsometric parameters are linear in γ^2 but are only marginally affected by η. This means that ellipticity and nonorthogonality defects in the laser beam incident on the interferometer (represented by η) have little influence on measurement accuracy and that polarization-state distortions due to imperfections in the PBS and other components in the interferometer arms (represented by γ) are much more important error sources.

According to Fig. 6 and Fig. 7, $\gamma \approx 0.03$ will produce

$$\delta\Delta \approx 0.1 \text{ deg}, \qquad \frac{\delta|\rho|}{|\rho|} \approx 0.1\% \tag{23}$$

Substitution of Eq. (23) into the fundamental ellipsometry equations[2] gives an error of thickness measurement of about 1 to 2 nm. Obviously, it is less than the experimental error shown in Table 1, on account of the simple error model adopted.

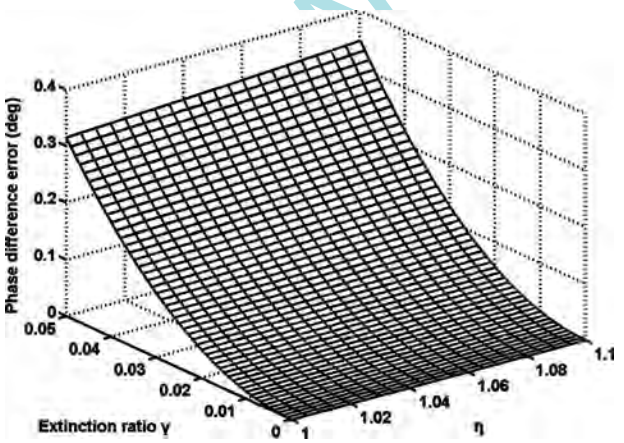

Fig. 7 Phase difference error versus η and γ.

Calibration is necessary to the obtain amplitude ratio; it helps to reduce the polarization mixing error of amplitude ratio according to Eq. (19) and Eq. (20). However a prerequisite assumption was made in those equations that the error parameters γ and η do not alter during the measurement process. In fact they vary a little with atmospheric conditions.[20] Therefore the real amplitude ratio error shown in Table 1 is more than the theoretical result in Fig. 6.

A heterodyne interferometer usually uses orthogonally polarized beams in its reference and measurement arms, which are separated by a PBS. But the system presented here does not. So the error resulting from the elliptical polarization and nonorthogonality of the light beams before BS1 is significantly smaller than in an interferometric reflection ellipsometer using a Zeeman laser.[21] The system shown in Fig. 1 only produces second-order error and should have more application potential.

6 Conclusion

A heterodyne interferometric transmission ellipsometer using two acousto-optical modulators has been presented. Without any rotating mechanical parts, the measurement system is expected to operate at high speed and stability. The symmetric configuration helps to improve the antiinterference performance, so the system is more applicable to *in situ* and real-time measurement than conventional ellipsometers. An error of several nanometers in film thickness measurement is observed; the repeatability is limited by the polarization mixing error.

A full analysis based on the Jones matrix method has been carried out on the polarization mixing error in terms of the imperfection and misorientation of the PBS and the elliptical polarization and non orthogonality of the light beam. The error is mainly introduced by γ. The elliptical polarization and non orthogonality resulting from the laser source and the half-wave plate are less important.

In fact, the error parameters γ, b, and ε vary a little with environmental conditions.[20] Therefore, the polarization mixing error always appears as a quasi periodic drift. Although the drifting behaviour of the error is not studied in this paper, the results are expected to be useful when artificial intelligence, such as neural networks and genetic algorithms, is applied to compensating and eliminating the error.[22]

Acknowledgments

The authors would like to thank Prof. Ji-bin Li and his graduate student Fei Luo for their help in using an atomic force microscope, and Prof. Jian-quan Yao for beneficial discussion. Funding by the ShenZhen Science & Technology Program (No. 200721) is gratefully acknowledged.

References

1. O. Auciello and A. R. Krauss, *In Situ Real-Time Characterization of Thin Films*, Wiley, New York (2001).
2. R. M. A. Azzam and N. M. Bashara, *Ellipsometry and Polarized Light*, North-Holland, Amsterdam (1977).
3. M. G. Boudreau, S. G. Wallace, G. Balcaitis, S. Muragkar, H. K. Haugen, and P. Mascher, "Application of in situ ellipsometry in the fabrication of thin-film optical coatings on semiconductors," *Appl. Opt.* **39**(6), 1053–1058 (2000).

4. K. Hemmes, M. A. Hamstra, K. R. Koops, M. M. Wind, T. Schrom, J. de Laet, and H. Bender, "Evaluation of interferometric ellipsometer systems with a time resolution of one microsecond and faster," *Thin Solid Films* **313–314**, 40–46 (1998).
5. C.-h. Lin, C. Chou, and K.-s. Chang, "Real time interferometric ellipsometry with optical heterodyne and phase lock-in techniques," *Appl. Opt.* **29**(34), 5159–5162 (1990).
6. H. F. Hazebroek and W. M. Visser, "Automated laser interferometric ellipsometry and precision reflectometry," *J. Phys. E* **16**, 654–661 (1983).
7. H. F. Hazebroek and A. A. Holscher, "Interferometric ellipsometry," *J. Phys. E* **6**, 822–826 (1973).
8. M. M. Wind and K. Hemmes, "New ultra-fast interferometric ellipsometry system based on Zeeman two-frequency laser," *Meas. Sci. Technol.* **5**, 37–46 (1994).
9. M.-H. Chiu, J.-Y. Lee, and D.-C. Su, "Complex refractive-index measurement based on Fresnel's equations and the use of heterodyne interferometry," *Appl. Opt.* **38**(19), 4047–4052 (1999).
10. L. R. Watkins and M. D. Hoogerland, "Interferometric ellipsometer with wavelength-modulated laser diode source," *Appl. Opt.* **43**(30), 4362–4366 (2004).
11. C.-m. Wu and C.-s. Su, "Nonlinearity in measurements of length by optical interferometry," *Meas. Sci. Technol.* **7**, 62–68 (1996).
12. W. Hou and G. Wilkening, "Investigation and compensation of the nonlinearity of heterodyne interferometers," *Precis. Eng.* **14**, 91–98 (1992).
13. J. M. De Freitas, "Analysis of laser source birefringence and dichroism on nonlinearity in heterodyne interferometry," *Meas. Sci. Technol.* **8**, 1356–1359 (1997).
14. J. M. De Freitas, "Phase nonlinearity extrema in Zeeman heterodyne interferometry," *Opt. Eng.* **39**(2), 572–575 (2000).
15. T. B. Eom, T. Y. Choi, K. H. Lee, H. Choy, and S. Lee, "A simple method for the compensation of the nonlinearity in the heterodyne interferometer," *Meas. Sci. Technol.* **13**, 222–225 (2002).
16. C. Yin, G. Dai, Z. Chao, Y. Xu, and J. Xu, "Determining the residual nonlinearity of a high-precision heterodyne interferometer," *Opt. Eng.* **38**(8), 1361–1365 (1999).
17. H. Zhao and G. Zhang, "Nonlinear error by orientation and elliptic polarization in a two-beam interferometer," *Opt. Eng.* **41**(12), 3204–3208 (2002).
18. B. Li and J.-w. Liang, "Effects of polarization mixing on the dual-wavelength heterodyne interferometer," *Appl. Opt.* **36**(16), 3668–3672 (1997).
19. S. Y. Lee, J. F. Lin, and Y. L. Lo, "Measurements of phase retardation and principal axis angle using an electro-optic modulated Mach-Zehnder interferometer," *Opt. Lasers Eng.* **43**, 704–720 (2005).
20. G. L. Dai, C. Y. Yin, and G. P. Xie, "Study on drift of nonlinearity in nanometer precision heterodyne interferometers," *Acta Opt. Sin.* **18**, 1697–1702 (1998).
21. Y.-l. Deng, X.-j. Li, Y.-b. Wu, J.-g. Hu, and J.-q. Yao, "Analysis of frequency mixing error on heterodyne interferometric ellipsometry," *Meas. Sci. Technol.* **18**(11), 3339–3343 (2007).
22. Z. Li, K. Herrmann, and F. Pohlenz., "A neural network approach to correcting nonlinearity in optical interferometers," *Meas. Sci. Technol.* **14**, 376–381 (2003).

Yuanlong Deng graduated from the Department of Precision Instruments of Tsinghua University, and received his PhD degree in 2007 from Tianjin University. He has been at ShenZhen University, where he is an associate professor, since 1997. His research interests include nanometer heterodyne interferometers, sensors and sensing, and artificial intelligence.

Jinlong Chai received his MS from Hua-Zhong University of Science and Technology. He works as an associate professor in the College of Mechatronics & Control Engineering of ShenZhen University. His main research interests are mechanical design, solar cells, and optical testing.

Xuejin Li received his PhD degree in optoelectronics from Tianjin University of China. He serves as a professor in the College of Physical Science and Technology of ShenZhen University. His research interests focus on optical fiber sensors. He has published more than 30 papers.

Yubin Wu graduated from Shenzhen University in 1994, and received his master's degree in 2004 from Southwest Jiaotong University of China. He has been at ShenZhen University, where he is an associate professor, since 1995. His research interests include visual servos, sensors and sensing, and artificial intelligence.

Gang Xu received his PhD degree from Nanjing University of Aeronautics and Astronautics in 1995. From 1996 to 1997, he was a postdoctoral fellow at Sussex University, UK. He worked as an invited scholar at Louisiana State University, USA, from 1987 to 1989. Since 1998, he has been at ShenZhen University, where he is a professor and serves as the dean of the College of Mechatronics & Control Engineering. His research interests are in the areas of intelligent control, machine vision, and automation engineering.